Cost effective microwave generation and detection system for qubits

Renato Bellotti

Supervisor: Dr. Sébastien Garcia
Quantum Device Lab at ETH Zürich
Prof. Dr. Andreas Wallraff

October 8, 2017

Abstract

This report describes how the relatively cheap Vaunix Lab Brick LMS103 microwave generators can be used for qubit spectroscopy of a superconducting transmon qubit. The characteristics of the devices are explained and a new measurement setup is developed. This new setup allows to successfully measure the eigenstates of the coupled qubit-cavity system. Though the new setup should theoretically be able to realise Rabi oscillations, they could not be realised due to time constraints and insufficient qubit quality.

Contents

1 Introduction, Goals and Motivation **3**

2 Theoretical background: Transmon qubit **4**
2.1 Qubit 4
2.2 Transmon qubit 4
2.2.1 Energy in a SQUID loop 4
2.3 Transmon qubit inside a cavity 6
2.4 Measurement of a transmon qubit 7

3 Characterisation of the LMS103 MW generators **9**
3.1 Data sheet values 9
3.2 Measured values 10
3.2.1 Power output 10
3.2.2 Need for external reference 10
3.2.3 Heat up effects and phase stability 11

4 Experimental Methods and Setup **14**
4.1 Planned approach 14
4.2 Usual setup 14
4.2.1 Coarse sketch of the idea 14
4.2.2 Realisation of the frequency sweep 14
4.3 Problems with the usual setup 16
4.4 New setup 16

5 Results **18**
5.1 Spectroscopy 18
5.2 Rabi oscillations and qubit lifetime 19

6 Conclusion and Outlook **21**

A Influence of phase instability on the intermediate signal of a mixer **23**

1 Introduction, Goals and Motivation

Figure 1: A Vaunix LMS103 Lab Brick generator.

The goal of this work was to use two Vaunix Lab Brick LMS103 microwave generators (depicted in Fig. 1) to perform qubit spectroscopy on a superconducting transmon qubit. The reason for this was that they offer reasonable power while being relatively cheap. In fact, their price is about a factor 3 smaller compared to the microwave generators currently in use in the lab.
The ability to prepare, manipulate and read out qubit states at low costs will become more and more important when the systems are scaling up to several qubits.

The following work was done during the thesis:

- Gain knowledge about the theoretical foundations of transmon qubits.
- Measure the properties of both used Lab Brick microwave generators.
- Test if the usual setup works together with the Lab Bricks. It does not.
- Develop a new setup.
- Perform cavity spectroscopy using the new setup.
- Realise Rabi oscillations.

2 Theoretical background: Transmon qubit

2.1 Qubit

The fundamental piece of information in a classical computer is a bit: It represents one of the values 0 or 1 [1]. Similarly, the fundamental information unit in quantum information theory is the qubit. Its state can be an arbitrary superposition of the states $|0\rangle$ and $|1\rangle$:

$$|\Psi\rangle = c_1 |0\rangle + c_2 |1\rangle , \tag{1}$$

where $|\Psi\rangle$ is the state of the qubit and the coefficients $c_1, c_2 \in \mathbb{C}$ fulfil the normalization condition

$$\langle\Psi|\Psi\rangle = |c_1|^2 + |c_2|^2 = 1, \tag{2}$$

in order to preserve the interpretation of the coefficients as probability amplitudes.
Altogether, a qubit is a quantum mechanical 2-state-system. There are several ways to implement such a system in practice, e. g. using quantum dots, photon states, trapped ions or superconducting materials [2]. For the measurements discussed in this report, only superconducting qubits (transmon qubits, see next section) were used.

2.2 Transmon qubit

A transmon qubit is a superconducting resonant circuit. Basically, it is a non-linear LC circuit [3]:
A pure LC circuit corresponds to a harmonic quantum oscillator. This means that all energy eigenvalues are equally spaced. In a harmonic oscillator, only coherent states can be produced. This means that it is not possible to excite one energy eigenstate without exciting the others.

Therefore, an anharmonic part is added by replacing the inductor L with a SQUID (Superconducting Quantum Interference Device). This causes the energy levels of the higher excited states to rise, making it possible to neglect them because they will never be excited in the experiment. The SQUID itself consists of two Josephson junctions connected in parallel. A Josephson junction is at cryogenic temperatures a non-linear non-dissipative inductor.
Putting the pieces together, one arrives at the schematic of the Transmon qubit, depicted in Fig. 2.

2.2.1 Energy in a SQUID loop

A branch is the set of elements between two nodes in an electromagnetic circuit. The branch flux of a Josephson junction $\Phi(t)$ and the current through

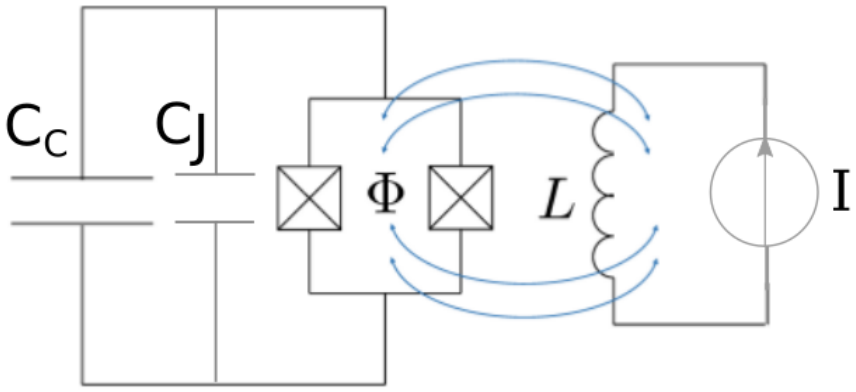

Figure 2: Circuit diagram of a transmon qubit. The two Josephson junctions (square with cross inside) form a SQUID. The flux through it is controlled by the external coil L. The SQUID and the capacitor C_C form the transmon qubit. The capacitor C_J accounts for the capacitive contribution of the Josephson junctions. [5], [4]

it $I(t)$ are given by [3]:

$$\Phi(t) := \int_{-\infty}^{t} V(t')dt' \tag{3}$$

$$I(t) = I_0 \sin\left(\frac{2\pi\Phi(t)}{\Phi_0}\right), \tag{4}$$

where $V(t)$ is the difference of electrical potential along the junction, $\Phi_0 = \frac{h}{2e}$ the flux quantum and I_0 the critical current of the Josephson junctions. h is the Planck constant and e the electrical elementary charge.

Using Equ. 3, Equ. 4 and the fact that the electromagnetic power performed at time t' is given by $V(t')I(t')$, it can be shown that the energy stored in the junction is given by the following formula:

$$\begin{aligned} E(t) &= \int_{-\infty}^{t} dt' V(t')I(t') = \int_{-\infty}^{t} \frac{d\Phi(t')}{dt'} I_0 \sin\left(\frac{2\pi\Phi(t')}{\Phi_0}\right) dt' \\ &= -E_J \cos\left(\frac{2\pi\Phi(t)}{\Phi_0}\right), \end{aligned} \tag{5}$$

where $E_J := \frac{\Phi_0}{2\pi} I_0$ is the Josephson energy.

The Coulomb charging energy is the energy stored in the capacitor. It is given by

$$E_{C_\Sigma} := \frac{(2e)^2}{2C_\Sigma}, \tag{6}$$

where $C_\Sigma = C_C + C_J$ is the total capacitance consisting of the contributions of the capacitor C_C and the capacitive part of the Josephson junctions C_J.

The Hamiltonian of the SQUID device can now be written as follows [5]:

$$H = E_C(n - \frac{Q_r}{2e})^2 + E_J \cos(\theta) \tag{7}$$

In the above equation, $n := \frac{q}{2e}$ is the number of charge carriers, Q_r the residual offset charge on the capacitor C_C (see Fig. 2), ϕ_{ext} the magnetic flux caused by the external coil and θ is the phase difference between the superconducting materials on both sides of the Josephson junctions. The electric energy arising from the current through the Josephson junctions E_I is given by

$$E_I = E_I(\Phi_{\text{ext}}) = E_{I_0} \left| \cos\left(\frac{2\pi\Phi_{\text{ext}}}{\Phi_0} \right) \right|, \tag{8}$$

where E_{I_0} is the maximum energy that can be stored in the current through the Josephson junctions and Φ_{ext} is the external magnetic flux through the junctions.
Finally, it can be shown that the frequency of a transmon qubit is proportional to $\sqrt{8E_I E_C} - E_C$ and can therefore be tuned by adjusting the external magnetic flux Φ_{ext} [4].

2.3 Transmon qubit inside a cavity

To prevent the qubit from randomly radiating energy and decaying while doing so, it is put inside a cavity.
A perfect empty cavity only allows certain electromagnetic modes in the inside. However, the presence of a qubit changes these allowed modes. This can be explained by considering the quantum mechanical framework: The "allowed" modes of the mixed photon-qubit system are the eigenstates of the Hamiltonian of the system. The latter one consists of three contributions:

1. **Electromagnetic field**:
   From quantizing the electromagnetic field, one knows that the Hamiltonian of a photon with frequency ω_0 is the one of a harmonic oscillator with frequency ω_0 [6]. Neglecting the energy of the vacuum, it is given by
   $$H_{EM} = \hbar\omega_0 a^\dagger a.$$
   Note that $a^\dagger$ is the creation operator and a the annihilation operator of the photon field.

2. **Qubit:**
   The Hamiltonian of a 2-level-system can be written as
   $$H_Q = \frac{1}{2}\hbar\omega_q \sigma_z,$$
   where ω_q is the frequency of the qubit.

3. **Coupling term**:
   Define the coupling constant g. It describes the strength of the coupling between the cavity and the transmon qubit [5]. Applying the rotating wave approximation, the Hamiltonian describing the coupling of the electromagnetic field to the cavity can be written by the following formula [5]:
   $$H_{coupling} = \hbar g(\sigma_+ a + \sigma_- a^\dagger)$$

The resulting Hamiltonian is called the Jaynes-Cummings Hamiltonian (JC Hamiltonian) [5]:

$$H = \frac{1}{2}\hbar\omega_q(B)\sigma_z + \hbar\omega_0 a^\dagger a + \hbar g(\sigma_+ a + \sigma_- a^\dagger) \tag{9}$$

The eigenvalues of the Jaynes-Cummings Hamiltonian can be calculated as follows [7]:

$$E_\pm = \hbar\omega_0 + \frac{1}{2}\hbar\left(\Delta \pm \sqrt{\Delta^2 + 4g^2}\right), \tag{10}$$

where $\Delta(B) = \omega_q(B) - \omega_0$ is the detuning parameter of the coupled system. Equ. 10 holds only for the subspace that preserves the total energy of the qubit-cavity system, $\{|g,1\rangle, |e,0\rangle\}$, where $0, 1$ denote the excited states of the EM field (i. e., the number of photons in the cavity) and e, g the states of the qubit. The term $\hbar\omega_0 + \frac{1}{2}\hbar\Delta = \frac{1}{2}\hbar(\omega_0 + \omega_q(B))$ is the total energy in the system when there is no coupling between the qubit and the electromagnetic field. One can see that at resonance ($\Delta = 0$), the energy-eigenvalues are shifted by $2g$ compared to the case without coupling.

2.4 Measurement of a transmon qubit

For small detuning $|\Delta| \approx 0$ (i. e. resonance), the difference between both energy eigenstates, $E_+ - E_-$, is equal to $2g$, see Fig. 3. It is therefore possible to determine the value of the coupling constant g by measuring the splitting between both eigenvalue curves. This method is called cavity spectroscopy: Only one microwave generator is needed.
After that, so called two tone spectroscopy is performed. There, the cavity is driven at resonance, but an additional microwave generator probes the qubit. This generator performs a sweep in a region where the detuning is large, $|\Delta| >> 0$. The resulting measured transmission curve of the cavity is shifted in frequency (dispersive shift). Because the direction of this shift depends on the qubit state, this can be used to determine the state of the qubit.

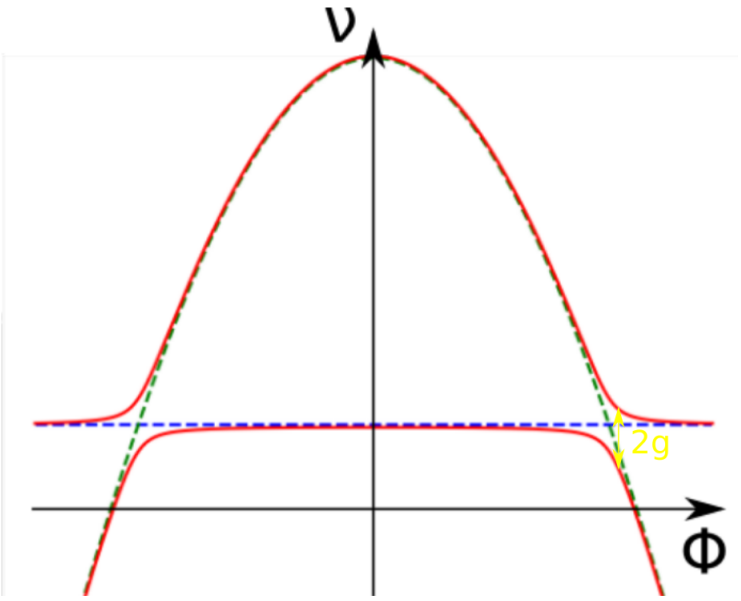

Figure 3: Splitting of the eigenvalues. ν is the transition frequency of the qubit, Φ the external magnetic flux. The blue curve denotes the eigenfrequency of the cavity without the qubit. The green curve represents the eigenfrequencies of the transmon qubit. Finally, the eigenfrequencies of the coupled system are depicted as the red curves.

3 Characterisation of the LMS103 MW generators

Figure 4: A Vaunix Lab Brick LMS 103 microwave generator.

The setup described in section 4 of this report uses two microwave generators. It is necessary to briefly summarize the properties of both of them in order to follow the further development of the spectroscopy setup. The generators will be referred to by the corresponding serial number, i. e. SN2573 and SN2574.
A picture of a Lab Brick microwave generator is shown in Fig. 4.

3.1 Data sheet values

According to the data sheet [8], the values of the properties that are most important for our needs are:

- **Frequency range:**
  5 - 10 GHz, with a resolution of 100 Hz, a switching time of 100 μs and an accuracy of $\pm$2 PPM
- **Power range:**
  -40 - +10 dBm
- **External reference:**
  the usual 10 MHz BNC reference clock or a built-in clock
- **Physical connectors:**
  SMA-female for the microwave output, BNC for the external reference clock, USB for power and controlling it with a computer

- **Software control:**
  LabView library and GUI are available.

3.2 Measured values

3.2.1 Power output

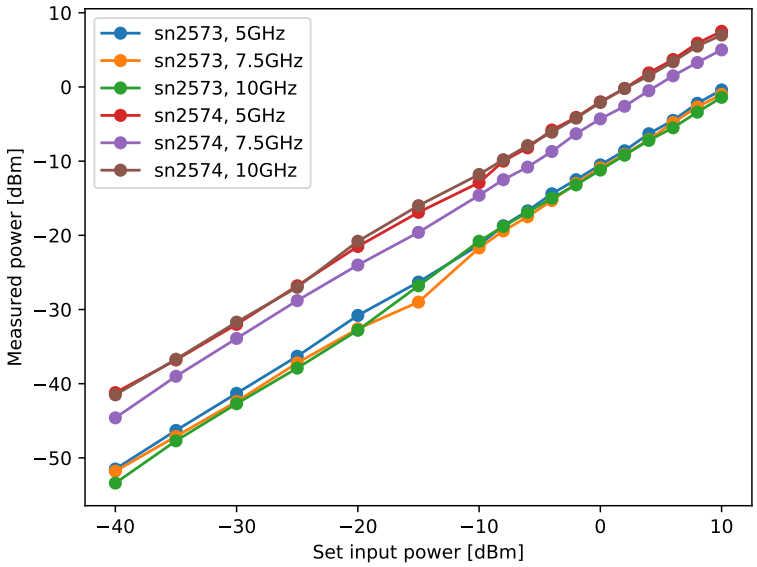

Figure 5: The power output of the used Lab Brick LMS103 microwave generators vs. set values.

The power output of both generators is lower than the one in the specification. A detailed plot can be found in Fig. 5. The measured curve is still linear. This means that the deviation from the specified power behaviour is just an offset. This can be compensated by using amplifiers. Other than that, there is no need for compensation.
The used microwave generators were used in the lab some years ago. Perhaps they were mishandled (e. g. too much power was reflected back to the outputs) and took damage. It is therefore not clear whether the offset is inherent to the model Lab Brick LMS 103 or if just the examined devices are broken.

3.2.2 Need for external reference

Measurements have shown that the internal clock of the Lab Bricks is not precise. One of the plots for the SN2574 is depicted in Fig. 6. It compares the power output of the microwave generator using its internal reference

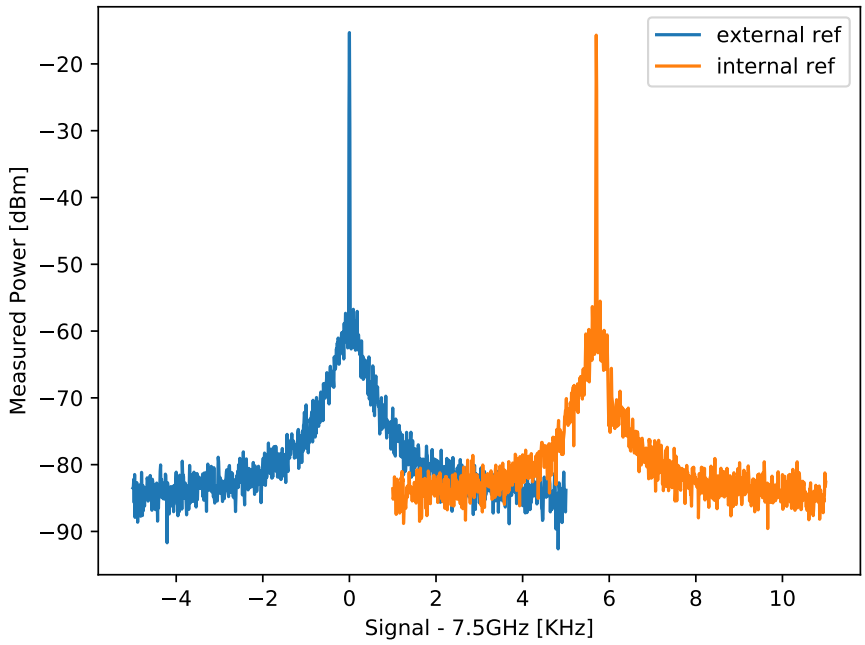

Figure 6: Power output of the Lab Brick SN2574 generator as a function of the frequency. The frequency was fixed at 7.5 GHz (0 of the graph), while the power output was set to -10 dBm (corresponds to physical power of approximately -15 dBm) via the LabView interface.

clock to the output taken with an external 10 MHz Ru clock. The signal using the internal clock is shifted in frequency by approximately 6 kHz compared to the desired value. In the corresponding plots for the SN2573 (not shown), the curves taken with internal and external references overlap, but an external reference was nevertheless used during all other measurements in order to guarantee proper operation.
Also note that the jitter in frequency, which can be read from the "thickness" of the curve, is the same for both the internal and external reference. Therefore, the external reference only locks the signal to the correct frequency, but does not affect the limits of frequency stability.

3.2.3 Heat up effects and phase stability

The phase shift of the generator with respect to the reference clock was examined. The measurement setup is depicted in Fig. 7: A mixer subtracts the frequencies of the two examined generators (both using the same 10 MHz reference clock), which yields a 10 MHz signal. The phase of this signal is

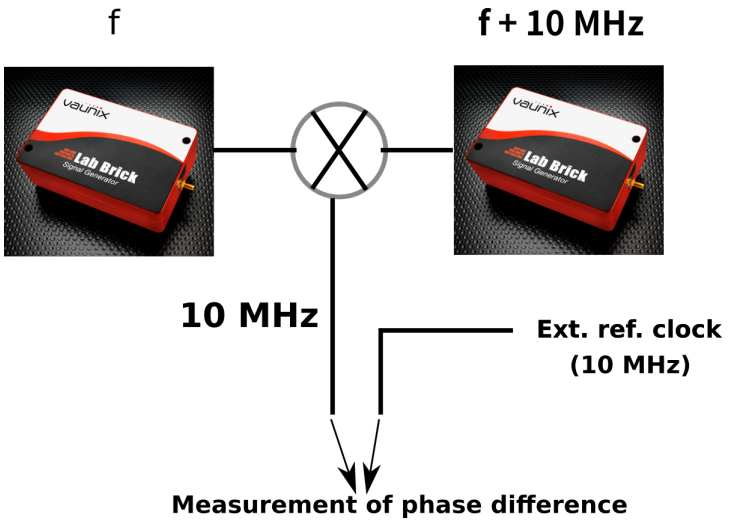

Figure 7: The measurement setup used to examine the phase properties of the Lab Brick generators.

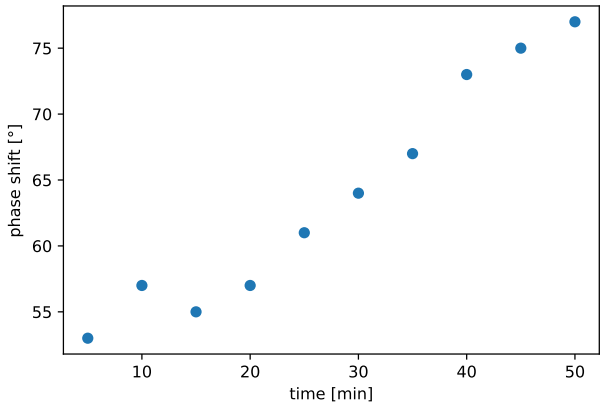

Figure 8: Phase shift depending on time. The reason for this behaviour is that the generator heats up.

then compared to the phase of the used reference clock.
The result is shown in Fig. 8. The phase shift increases clearly with time. It was measured again after letting the Lab Brick run for 2 days. Then, it was stable. It is thus legitimate to consider the curve in Fig. 8 as a heat up effect. This agrees with the observation that the temperature of the microwave generators is significantly higher than the temperature in the lab.
The phase stability is depicted in Fig. 9. It is never lower than approximately 6.7 degrees. This might be a problem and will be discussed in more detail

in section 4.3 and in appendix A.
For these effects, a setup was picked that is independent of the phase and frequency stability of the microwave generator.

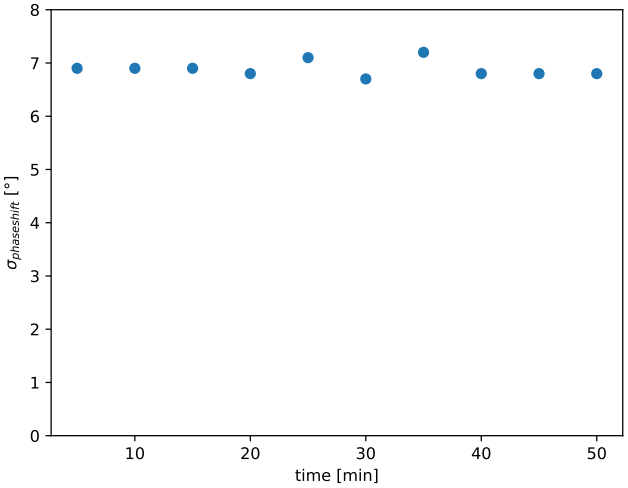

Figure 9: Phase instability of the Lab Bricks, i. e. standard deviation of the phase shift.

4 Experimental Methods and Setup

The goal of this semester thesis is to measure a cavity-transmon system. This is done by measuring the splitting of the two eigenenergies of the coupled system consisting of a photon and the qubit. The splitting is depicted in Fig. 3 (see section 2.4 for more details and discussion).
Spectroscopy is performed by sending microwaves through the cavity at cryogenic temperatures and measure the transmission spectrum. The measured intensity can then be mapped to different colours. The region with highest intensity should have approximately the same shape as the red curves in Fig. 3.

4.1 Planned approach

The qubit is placed in a cavity and cooled down to cryogenic temperatures. Its frequency will be tuned by controlling the magnetic flux using an external coil. Then Lab Brick devices will be used to generate a microwave signal. The transmission spectrum is then digitised and stored on a regular computer.
Microwaves are used because all available cavities are designed to work in the microwave regime.
The transmission spectrum will depend on the qubit frequency and state (see Equ. 10 and discussion). This comes from the fact that the coupling between qubit and cavity leads to a splitting of the eigenergies of the system. The energy levels are shifted depending on the state of the qubit.
The spectrum is recorded on a computer. Since the available cavity has a frequency of 7 GHz, it is necessary to generate a signal in this regime. But at the current state of technology, it is very hard and expensive to digitise a signal in the regime of approximately 7 GHz using a regular computer (clocked at approximately 3 GHz). Therefore, mixers are used to downconvert the signal to the MHz regime, which can be measured.

4.2 Usual setup

4.2.1 Coarse sketch of the idea

An external coil is used to tune the qubit transition frequency. For each value of the magnetic field Φ, a frequency sweep is performed. For each of these configurations, the transmitted intensity is measured.

4.2.2 Realisation of the frequency sweep

The signal to drive the cavity is generated by a Lab Brick microwave generator and sent through the cavity. Theoretically, the signal is only transmitted if it hits one of the eigenfrequencies of the coupled system. But in practise,

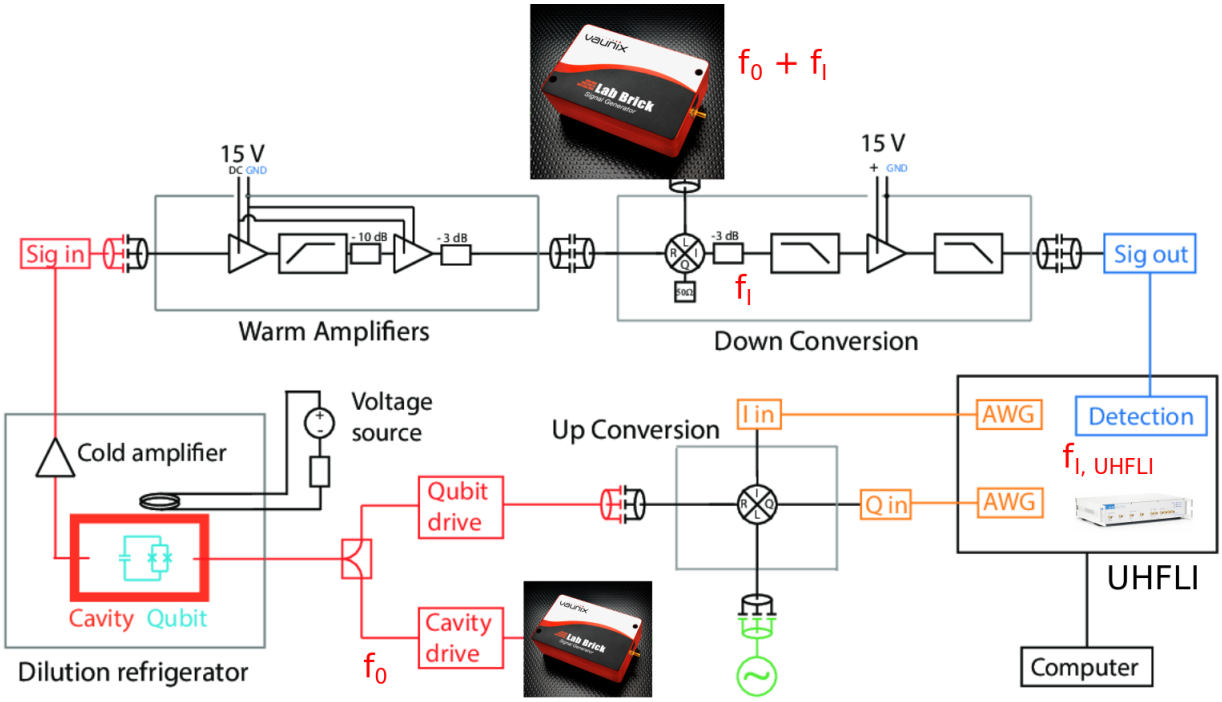

Figure 10: The usual spectroscopy setup. [9]

neither the cavity nor the qubit is perfect. Because of that, the transmitted intensity follows a Loretzian, i. e. a resonance curve, centred around the eigenfrequencies.
Because the transmitted signal has low intensity, amplifiers have to be used. Each amplifier adds noise to the signal. In order to minimise this noise, the first amplifier is placed inside the dilution refrigerator. Afterwards the signal is carried outside out the dilution refrigerator. There it is filtered and amplified again. Afterwards the signal must be down converted. The reason for this is the following: The goal of this experiment is real time qubit spectroscopy, so the signal has to be processed at short time scales. But digitisation of a GHz signal cannot be done at the current stage of technology without expensive oscilloscopes. In order to keep costs low, the signal is down converted using a mixer. The low frequency signal is then digitized by an FPGA-based Zurich Instruments UHFLI.
The UHFLI is also used to drive the qubit. Because the same device is used both for measurement and driving, the Zurich Instruments generator is in fact used as a lock-in amplifier. The advantage of this is that it allows to realise Rabi oscillations and therefore manipulate the state of the qubit.

4.3 Problems with the usual setup

The Lab Brick microwave generators cannot be used in the conventional setting (described in section 4.2) because of the insufficient frequency resolution of the Lab Brick generators:
A priori, there are two possible problems with the Lab Bricks: Phase fluctuations and limits of frequency resolution. It can be shown (see appendix A for detailed calculation) that the phase fluctuations do not represent an obstacle to use the planned setup: The amplitude $A_{\text{measured}} = Ae^{-2\sigma^2}$ is exponentially suppressed compared to the amplitude without phase fluctuations A. For the measured phase instability of approximately 7 degrees, the relative amplitude compared to the ideal signal without phase fluctuations is given by $\frac{A_{\text{measured}}}{A} \approx 78.3\ \%$. This can be compensated by using amplifiers. The signal is phase shifted, but the shift is constant in time, $\varphi_{\text{measured}} = \text{const}$. This means there are no distortion effects due to phase fluctuations.
The main problem is therefore the insufficient frequency resolution: A measurement takes about 1 s of time to complete, which means that the frequency resolution should be better than approximately 1 Hz in order to avoid interference effects. But the Lab Bricks only offer resolution of approximately 100 Hz. This makes it impossible to downconvert the signal from the cavity with a different device than the one used for the upconversion: Due to the limited frequency resolution, $f_{\text{I}} \neq f_{\text{I,UHFLI}}$.
Because of these reasons it is not possible to use the conventional setup with the Lab Brick generators. Instead, a new setup that is independent of limited frequency resolution will be used.

4.4 New setup

In the new setup, one of the Lab Bricks is used for cavity spectroscopy, the other one to drive the qubit directly.
The new setup for cavity spectroscopy is depicted in Fig. 11. The Lab Brick microwave generator serves as local oscillator with frequency f_0 (around 7 GHz) for both up and down conversion. The UHFLI MWG generates a sine wave at $f_{\text{UHFLI}} = 250$ MHz on output 1 and modulates it onto the microwave signal. The lower side band with frequency $f_0 - f_{\text{UHFLI}}$ is suppressed: The cables at the I and Q connections of the up conversion mixer are manually adjusted so that the phase shift between them leads to destructive interference. The resulting microwave is sent through the cavity. The transmitted signal is down converted and sent to the UHFLI input 1. There it is digitised and stored on a computer.

The signal for Rabi oscillations is generated by the UHFLI AWG at 300 MHz. It is emitted through output 2 of the Zurich Instruments UHFLI. The other Lab Brick device is used to up convert the signal.

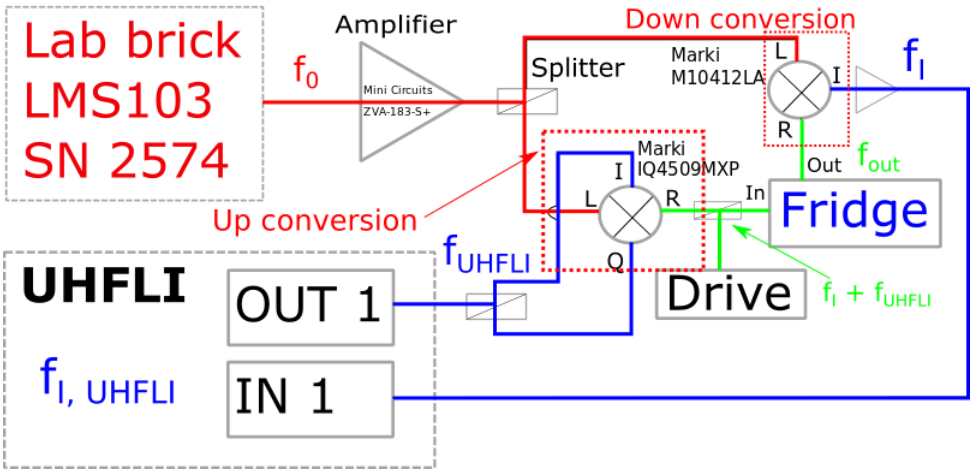

Figure 11: New spectroscopy setup using Lab Brick microwave generators. Notice that, in the up and down conversion, the lower side band with frequency $f_I - f_{\mathrm{UHFLI}}$ is strongly suppressed.

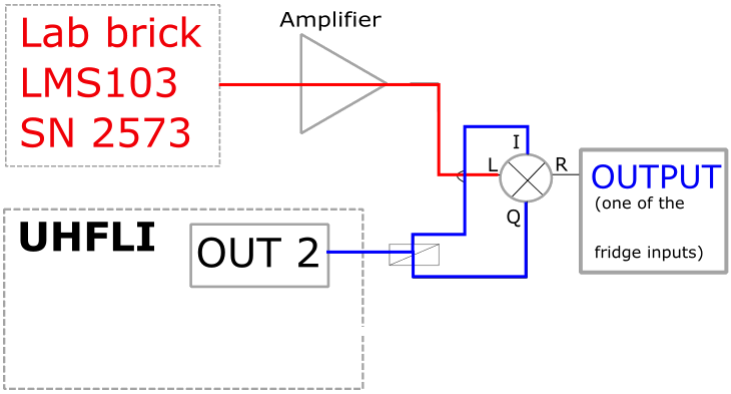

Figure 12: New setup for generating Rabi oscillations using Lab Brick microwave generators.

5 Results

5.1 Spectroscopy

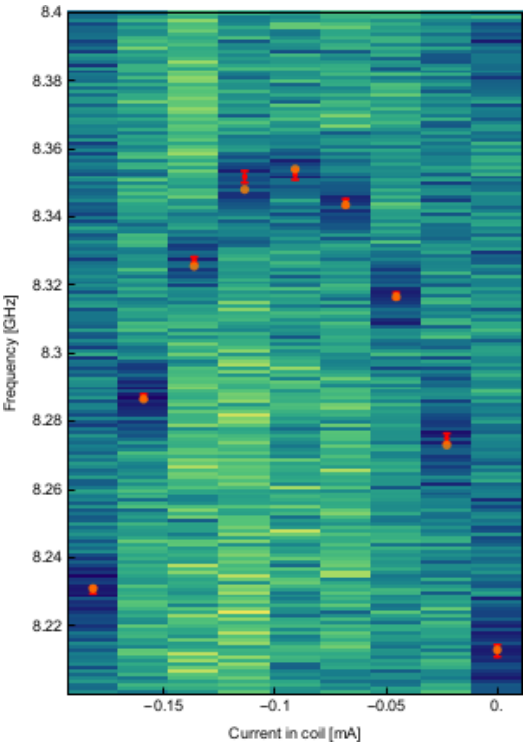

(a) The measured curve from two-tone spectroscopy.

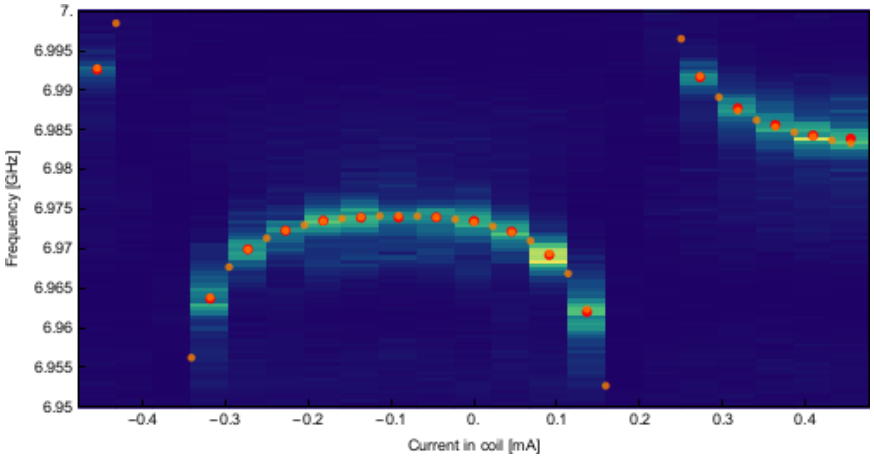

(b) The measured curve for cavity spectroscopy.

Figure 13: The measurement results.

It was possible to successfully perform cavity spectroscopy. A measurement is depicted in Fig. 13. The plots map the transmission intensity to colours. The horizontal axis shows the current through the coil, which determines the magnetic flux through the transmon qubit and therefore its frequency. The vertical axis represents the frequency of the incoming electromagnetic waves, i. e. of the Lab Brick signal.
First, the transmission around the cavity resonance was measured. The detuning for this measurement was small, $|\Delta| \approx 0$. This procedure is called cavity spectroscopy. The corresponding transmission spectrum is depicted in Fig. 13b. One can see that the curves of the eigenvalues have their maximum not for vanishing magnetic flux through the qubit: This effect is caused by other magnetic fields in the lab and leads to an offset magnetic flux Φ_{offset}.
Then, another measurement was performed. The cavity drive was set to resonance frequency and another Lab Brick was used to drive the qubit at large detuning, $|\Delta| >> 0$, close to its maximum frequency. Because two microwave generators are used independently, this method is called two-tone spectroscopy. The result of this measurement is depicted in Fig. 13a.
Then, a pseudo-fit was performed using the measured data from both measurements: The parameters of the theoretical curve were adjusted manually until a good overlap with the measured values was reached. In Fig. 13a, 13b the centre frequencies of Lorentzian fits against the measurement data are depicted as red circles, while the eigenfrequencies of a coupled system with adjusted parameters (from the pseudo fit) are drawn as orange circles.
The following four physical quantities were adjusted to make the theoretical values match the measured ones: The Josephson energy E_J, the coupling constant g, the flux offset expressed in equivalent current Φ_{offset} and the period of the current through the external coil T_I. Assuming that $E_C = 292$ MHz·h, the following values were obtained from the pseudo fit: $E_J = 32.03$ GHz·h, $\frac{g}{2\pi} = 99$ MHz, $\Phi_{\text{offset}} = 0.094$ mA and $T_I = 1.154$ mA.

5.2 Rabi oscillations and qubit lifetime

The attempt to manipulate the state of the qubit by realising Rabi oscillations has failed. The main cause of the problems can be further localised by taking a look at the measurements of the qubit line width depicted in Fig. 14. One can see that the magnitude of the line width is approximately 20 MHz. This is important because the line width is inversely proportional to the lifetime of a qubit:

$$\tau_{\text{qubit}} = \frac{1}{2\pi \cdot \text{linewidth}} = \frac{1}{\kappa}$$

It can be concluded that a line width in the regime of 20 MHz corresponds to a qubit lifetime in the regime of 10 ns, which is very short. This explains the difficulties in realising Rabi oscillations: The qubit does not live long enough to be reliably manipulated.

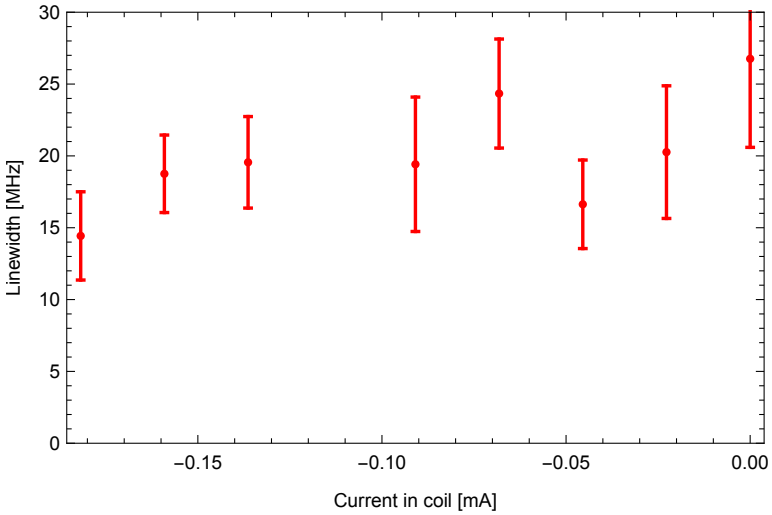

Figure 14: Measured line width of the qubit. The line width is depicted as $\frac{\kappa}{2\pi}$.

6 Conclusion and Outlook

This report has proven that it is possible to use Vaunix Lab Brick LMS103 microwave generators to perform qubit spectroscopy on a superconducting transmon qubit. The importance of this result comes from the fact that the overall price of a qubit has to be reduced in order to build multi-qubit quantum computers. The usage of the relatively cheap Lab Brick generators represents a further step towards economically feasible quantum computers. There were also problems. The biggest caveat of using Lab Bricks to replace more expensive microwave generators is their limited frequency resolution. It was not possible to manipulate the state of the qubit due to time constraints and because the quality (the lifetime) of the used transmon qubit was not good enough. The setup that was developed during this semester thesis should theoretically be able to successfully realise Rabi oscillations, given that a high quality transmon qubit is available. Further work should be invested to obtain such a qubit. Afterwards, it should be possible to empirically verify that the new setup is suitable to manipulate the state of a qubit.

The long-time goal of this semester thesis was to reduce the costs to implement a transmon qubit. The most expensive part of the whole measurement setup is, however, the Zurich Instruments UHFLI. This multi-purpose device is very versatile. But the fact that it can be used for various applications is also a big caveat: The UHFLI is very expensive. It could, in principle, be replaced by an FPGA, an ASIC and/or software defined radio device.

Acknowledgements

I want to thank the following people for their help during my work:
First of all my warmest thanks to Sébastien Garcia, my supervisor, who made this work even possible. When I applied for a thesis, I was a bit late, so all offered projects were already taken. But Sébastien couldn't stand to disappoint me, so he just created a new project, which is the one described in this report. He introduced me to the fascinating world of dilution refrigerators, microwave signal acquisition and processing and transmon qubits. Throughout the semester he kept the work interesting and varied by letting me do small workshop works when I was suffering from too much LabView problems.
Further, I want to thank Michele Collodo and Simon Storz for their unceasing effort in explaining the depths and quirks of LabView to me and helping me to include the new generators into the automated measurement setup and data acquisition software used in the lab (SweepSpot).
I want to thank Michele again, as well as Bruno, for their patience with my Zurich Instruments problems. I hope the next time you don't have to invest several weeks to find out that the computer is just too slow to receive high resolution data.
Last but not least I want to thank the whole Qudev group for including me in such a warm and open minded way. It was nice working side by side with you guys! I also want to thank Gaby Strahm for keeping our backs free from the terror of administrative tasks and allowing us to focus on our work.
Finally, I want to thank Prof. Dr. Andreas Wallraff for accepting my application and letting me work in this awesome group.

A Influence of phase instability on the intermediate signal of a mixer

We want to quantify the influence of a phase difference between the signals at the L and R inputs of a mixer in the signal at the I output:
The signals before the downconversion are:

$$\begin{aligned} S_R(t) &= \mathcal{A}_R e^{i\omega_R t} = A_R e^{i\Phi_R(t)} \\ S_L(t) &= \mathcal{A}_L e^{i(\omega_L t + \delta\Phi(t))} = A_L e^{i\Phi_L(t)}, \end{aligned} \tag{11}$$

where $A_R, A_L \in \mathbb{R}$.
After digital down conversion, the output signal looks as follows:

$$\begin{aligned} I_D \ \alpha \ Acos(\Phi_L - \Phi_R + \delta\Phi(t)) \\ Q_D \ \alpha \ Asin(\Phi_L - \Phi_R + \delta\Phi(t)), \end{aligned} \tag{12}$$

where $A := A_R A_L$.
The measurement result is averaged k times, so the relevant signal becomes:

$$< \mathcal{A}_D >_k = < I_D >_k + i < Q_D >_k \tag{13}$$

Assumptions:

- $\delta\Phi(t) = \delta\Phi_k = \text{const}$ during the time of averaging, i. e. during one acquisition
- The phase jitter follows a Gaussian distribution

  $$\rho(\varphi) = \frac{1}{\sqrt{2\pi}\sigma} e^{\frac{\varphi^2}{2\sigma^2}},$$

  where a new notation was introduced: $\varphi := \delta\Phi_k$. Also define $\theta := \Phi_L - \Phi_R$.

Now we can calculate the expectation values for I_D and Q_D:

$$\begin{aligned} < I_D > &= \int_{-\infty}^{\infty} I_D(\varphi)\rho(\varphi)d\varphi \\ &= \int_{-\infty}^{\infty} Acos(\theta+\varphi)\frac{1}{\sqrt{2\pi}\sigma} e^{-\frac{\varphi^2}{2\sigma^2}} \\ &= ... \\ &= Acos(\theta)e^{-2\sigma^2} \end{aligned} \tag{14}$$

Analogue, we arrive at:

$$< Q_D > = Asin(\theta)e^{-2\sigma^2} \tag{15}$$

Now we can combine Equ. 14 and Equ. 15 to the following two end results:

$$\bar{A} = |< A_I >| = \sqrt{< I_D >^2 + < Q_D >^2} = Ae^{-2\sigma^2} \tag{16}$$

$$\bar{\Phi} = \arctan\left(\frac{< Q_D >}{< I_D >}\right) = \theta \tag{17}$$

References

[1] E. Knill et al., *Introduction to Quantum Information Processing*, https://arxiv.org/abs/quant-ph/0207171

[2] Michael Brooks, *Quantum Computing and Communications*, Springer, 1999

[3] Vool, U., and Devoret, M. (2017) *Introduction to quantum electromagnetic circuits*. Int. J. Circ. Theor. Appl., 45: 897–934. doi:10.1002/cta.2359.

[4] Jens Koch et al., *Charge-insensitive qubit design derived from the Cooper pair box*, PHYSICAL REVIEW A 76, 042319 (2007), doi:10.1103/PhysRevA.76.042319

[5] Johannes Fankhauser, *Frequency-tunable Transmon qubit in a 3D copper cavity.*

[6] Robert Bennett et al., *A physically motivated quantization of the electromagnetic field*, European Journal of Physics, Vol. 37, Number 1, doi:10.1088/0143-0807/37/1/014001

[7] Christian Nietner, *Quantum Phase Transition of Light in the Jaynes-Cummings Lattice*, Freie Universität Berlin [Online], http://users.physik.fu-berlin.de/~pelster/Theses/nietner.pdf, retrieved on 05.09.2017

[8] Vaunix, *Lab Brick® LMS Signal Generators* [Online], retrieved on 23.08.2017, http://vaunix.com/datasheets/lms%20signal%20generators-datasheet.pdf

[9] Sébastien Garcia, *Proposal for a new advanced lab class experiment: Circuit Quantum Electrodynamics*, private communication

ETH

Eidgenössische Technische Hochschule Zürich
Swiss Federal Institute of Technology Zurich

Declaration of originality

The signed declaration of originality is a component of every semester paper, Bachelor's thesis, Master's thesis and any other degree paper undertaken during the course of studies, including the respective electronic versions.

Lecturers may also require a declaration of originality for other written papers compiled for their courses.

I hereby confirm that I am the sole author of the written work here enclosed and that I have compiled it in my own words. Parts excepted are corrections of form and content by the supervisor.

Title of work (in block letters):

Cost effective microwave generation and detection system for qubits

Authored by (in block letters):

For papers written by groups the names of all authors are required.

Name(s):	**First name(s):**
Belletti	Renato

With my signature I confirm that

- I have committed none of the forms of plagiarism described in the 'Citation etiquette' information sheet.
- I have documented all methods, data and processes truthfully.
- I have not manipulated any data.
- I have mentioned all persons who were significant facilitators of the work.

I am aware that the work may be screened electronically for plagiarism.

Place, date	**Signature(s)**
Urdorf, 08.10.2017	Renato Belletti

For papers written by groups the names of all authors are required. Their signatures collectively guarantee the entire content of the written paper.